JEE Journal of Ecological Engineering

Journal of Ecological Engineering 2023, 24(10), 369–379
https://doi.org/10.12911/22998993/170707
ISSN 2299–8993, License CC-BY 4.0

Received: 2023.07.19
Accepted: 2023.08.09
Published: 2023.08.24

Optimizing Electrodialytic Recovery of Mineral Ions from Bittern Wastewater Using D-Optimality Design

Anita Dwi Anggrainy[1], Afrah Zhafirah Sinatria[2], Arseto Yekti Bagastyo[1,2*], Zuhaida Mohd-Zaki[3]

[1] Research Center for Infrastructure and Sustainable Environment, Institut Teknologi Sepuluh Nopember, Surabaya 60111, Indonesia

[2] Department of Environmental Engineering, Institut Teknologi Sepuluh Nopember, Surabaya 60111, Indonesia

[3] Civil Engineering Studies, College of Engineering, Universiti Teknologi MARA, Cawangan Pulau Pinang, Permatang Pauh Campus, 13500 Pulau Pinang, Malaysia

* Corresponding author's e-mail: bagastyo@enviro.its.ac.id

ABSTRACT

Electrodialysis has been proven effective due to its high selectivity for separating monovalent and divalent ions. This study statistically evaluated the simultaneous electrodialytic recovery of mineral ions from bittern wastewater. The objective was to investigate the effect of cell number, anode materials, and applied voltage to optimize mineral ion recovery. A D-optimality design response surface methodology was performed to estimate the model parameter and identify the factors contributing to mineral ions recovery. The effects of independent variables and their interactions on the responses were investigated using ANOVA. All developed models were highly significant, with a *p*-value of <0.0001. The applied voltage was considered very important for the recovery process of all mineral ions as it affects the driving force of ion migration through the ion-exchange membrane. The optimization analysis (desirability value of 0.967) revealed 12% Cl^-, 14% SO_4^{2-}, 0.7% Mg^{2+}, and 21% Ca^{2+} recovery at the combination of 5-cells configuration, graphite electrode, and 9 V.

Keywords: bittern wastewater, D-optimality, electrodialysis, mineral recovery, response surface methodology.

INTRODUCTION

The salt production process releases a large quantity of bittern wastewater with a density between 29–30° Bé (ρ = 1.250–1.261) and salinity between 289.2–351.7 gL^{-1} at 25 °C (Dave and Ghosh 2005; Bagastyo et al. 2022). This wastewater is commonly disposed of in the nearby aquatic environment without further treatment considering the operational and maintenance costs (Ariono et al. 2016). Previous studies reported that long-term exposure to high salinity water could endanger marine organisms, e.g., seagrass, mangroves, coral reefs, clams, oysters, fish, green turtles, plankton, crabs larvae, and sea turtles (Einav et al. 2002; Tovar et al. 2002; Gacia et al. 2007; Roberts et al. 2010; Panagopoulos and Haralambous 2020).

Bittern contains a high concentration of minerals, such as chloride, magnesium, sodium, calcium, potassium, and sulfate (Dave and Ghosh 2005; Kartika and Bagastyo 2022) that can be recovered to increase their potential added value. The extraction of minerals from rejected brine or bittern wastewater has gained much interest in the past few decades. The recovery of minerals is typically carried out by nanofiltration, electrolysis, electrodialysis, precipitation, solvent extraction, ion exchange, or thermal operation (Bagastyo et al. 2021b). Those technologies can be used as a sole recovery treatment or combined to enhance recovery efficiencies.

In this study, electrodialysis was used to recover mineral ions from bittern wastewater. This technology employs the driving force of ionic exchange membranes to separate ions from the

solution (Strathmann 1986). Electrodialysis has advantages such as higher ion selectivity, low energy consumption, and a wide range of operational pH. It also has low waste by-products since fewer/no chemicals are required (Bagastyo et al. 2021a). Previous studies have proven that electrodialysis can be used to recover metals, minerals, or nutrients from various wastewater (Barakwan et al. 2019; Hikmawati et al. 2019; Mohammadi et al. 2021). Several parameters that may affect the performance of the electrodialysis process include temperature, flow rate, feed pH, salinity, current density, applied voltage, the concentration of coexisting ions, and the type of membrane (Nie et al. 2017; Ye et al. 2018; Zhang et al. 2020).

Apart from those parameters, the number of cells in the reactor configuration may also affect the efficacy process since it affects the membrane surface area and involves the recirculation process of feed water. To the author's knowledge, the effect of cell number and applied voltage on the process performance has rarely been statistically discussed. For this reason, this study aims to investigate the effect of cell number, anode materials, and applied voltage to optimize the recovery of mineral ions (e.g., Cl^-, SO_4^{2-}, Mg^{2+}, and Ca^{2+}). The experiments were performed using D-optimality design response surface methodology (RSM). The application of RSM could simplify the number of experimental runs, evaluate multiple parameters and their interaction with the response, and optimize the process (Wang et al. 2010). Moreover, the D-optimality design would search the candidates for the best design point and estimate the effects of the factors. Applying this method can identify the active factor that mostly drives the recovery process using a minimum number of experiments. In addition, specific energy consumption for each recovered mineral ion was also calculated for economic consideration.

MATERIAL AND METHODS

Bittern characteristics

Bittern wastewater was taken from a salt processing industry located in Surabaya, Indonesia. This wastewater is a residual stream of the salt washing process that uses brine (20–25 ºBé) as the washing water. The bittern characteristics are described in Table 1.

Table 1. Physico-chemical characteristics of bittern wastewater

Parameter	Unit	Concentration
pH	–	6.71
TDS	mg L^{-1}	57900
Cl^-	mg L^{-1}	87472.90
SO_4^{2-}	mg L^{-1}	399690
Na^+	mg L^{-1}	17.27
K^+	mg L^{-1}	8.92
Mg^{2+}	mg L^{-1}	373065
Ca^{2+}	mg L^{-1}	32130

The electrochemical process design

The experiments were carried out using acrylic reactors that consisted of 3-cell compartments (external dimension of 14 x 5 x 24 cm) and 5-cell compartments (external dimension of 14 x 8 x 24 cm), as seen in Figure 1. Each compartment was separated by ion exchange membranes, i.e., AMI-7001 or CEM-7000 (Membrane International Inc., USA), with a dimension of 14 x 24 cm (active surface area of 336 cm^2). Each experiment was conducted for 5 hours. Before experiments, the membranes were immersed in a 5% NaCl solution for 12 h for the pre-conditioning process. The anode comprises of platinum (Pt) and graphite plates, while the cathode is stainless steel (SS). The electrodes have an active surface area of 24 cm^2 (3 x 8 cm) each. The distance of electrodes was arranged at 2 cm for the 3-cell compartments and 6 cm for the 5-cell compartments. The experiment was performed galvanostatically using a 60 V/30 A DC power supply (Volomax KXN-6030D, China).

Analytical methods

All chemicals used in this process were analytical grade. The parameter analyses were duplicated and carried out according to the standard method (American Public Health Association 2005). A total of 100 mL samples were collected from each experiment and immediately filtered using a 0.45 μm syringe filter (ANPEL Technology, Shanghai, Inc.). The pH and TDS measurements were conducted using a handheld pH/TDS meter (YK-2005 WA, Lutron, Taiwan). The Cl^- and SO_4^{2-} ions were analyzed using argentometric Mohr and turbidimetric methods, respectively.

Additionally, the measurement of Mg^{2+} and Ca^{2+} ions was performed using the titrimetric

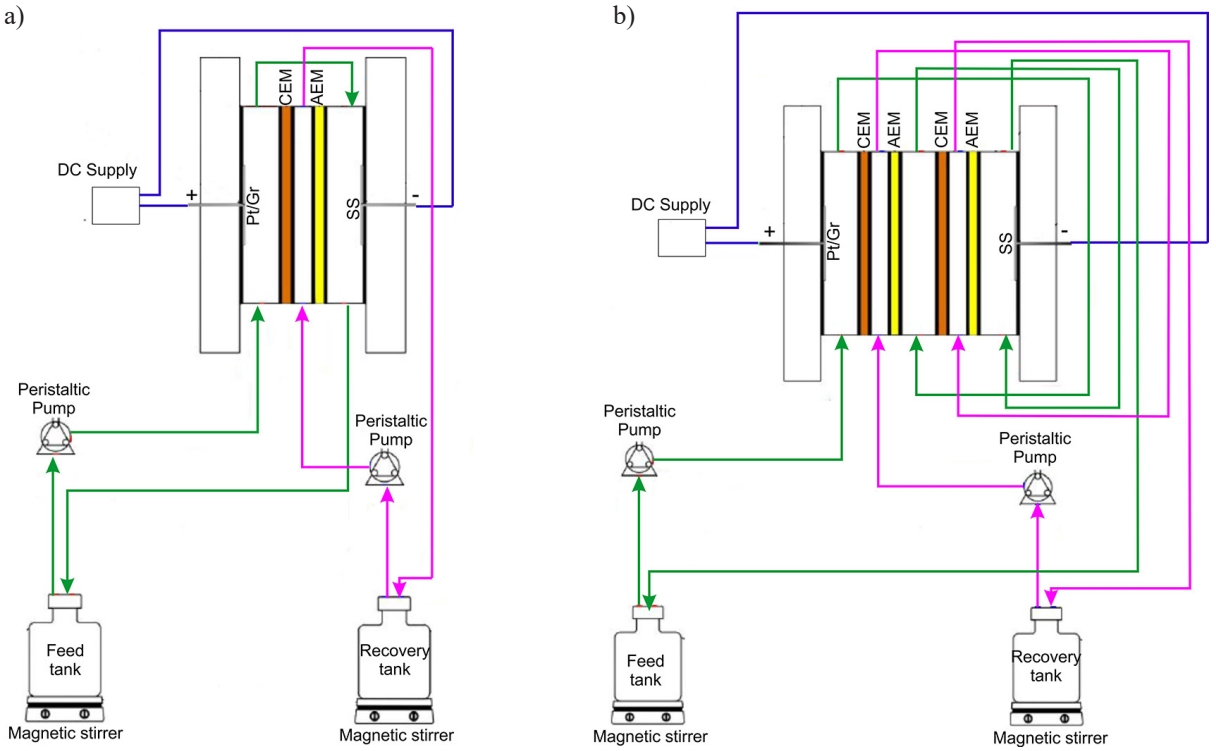

Figure 1. Experimental set-up: a) 3-cells electrodialysis reactor; b) 5-cells electrodialysis reactor

method. The concentration of COD was determined by the closed reflux and colorimetric method (Merck and Spectroquant NOVA), whereas the BOD_5 measurement was carried out by the titrimetric method and Winkler analysis. A scanning electron microscope-SEM (EVO MA10, Carl Zeiss) equipped with an energy dispersive x-ray (EDX) system was used to observe the morphology and characteristic of the recovered precipitates in the experiment.

Experimental design

The experiments and statistical analysis were conducted using Design Expert (version 11.1.2.0, Stat-Ease, Inc., USA). The individual factors of the model comprise of applied voltage (e.g., 3, 5, 7, 9 V), cell number (e.g., 3-cell and 5-cell), and electrode types (e.g., Pt and graphite). In this model, the applied voltage was set as a 4-level discrete numeric type, while the cell number and electrode type were sequentially set as 2-level ordinal and nominal categoric types. The ordinal scale was meant for a categorical variable with ordered categories, whereas the nominal scale is for a categorical variable without natural order (Agresti 2002). By default, the D-optimality required a minimum of 5 lack of fit points. However, the experimental design was set to 4 fit points and replicated to minimize the number of runs. Thus, a total of 20 runs were carried out in this study (i.e., 12 model points, four lack of points, and four replicate points). Statistical analysis was conducted using analysis of variance (ANOVA). The quality and significance of the developed models were determined using coefficient R^2, adjusted R^2, and the Fischer F-test. The p-value < 0.05 indicates that the term is significant.

Data analysis

The recovery efficiency of minerals was calculated as follows:

$$\eta\ (\%) = \frac{V_{ct}\ C_{r_t}}{C_0 - C_t} \times 100\% \qquad (1)$$

where: η (%) is the recovery efficiency of mineral ions;
C_0 (mg L^{-1}) is the initial concentration of a mineral ion in the feed solution;
C_t (mg L^{-1}) is the concentration of a mineral ion in the concentrated compartment;
C_{rt} (mg L^{-1}) is the concentration of a recovered mineral ion in the recovered tank;
V_{ct} (L) is the volume of the concentrate solution at time t.

RESULTS AND DISCUSSIONS

Recovery of mineral ions

Based on Figure 2, the overall recovery percentages can be ranked as follows: $Ca^{2+} > SO_4^{2-} > Cl^- > Mg^{2+}$. The recovery efficiency was substantially enhanced with the increased applied voltage and cell number. These results were in accordance with Honarparvar and Reible (2020), who revealed that increasing cell number could improve ion transport across the membrane by amplifying the residence time involved in salt fluxes and osmotic transport. These results also showed that graphite electrodes provide better ionic mobility than Pt due to their higher conductivity. Nonetheless, only 0.25–21.48% of targeted ions can be recovered from bittern wastewater, which was very low considering the removal of ions can be up to 93%, 61%, 86%, and 85% for Cl^-, SO_4^{2-}, Mg^{2+}, and Ca^{2+}, respectively. The lower recovery percentages of ions were likely because the recovery calculation only considered the dissolved ions and disregarded the readily formed precipitates in the electrode and membrane.

Model fitting and statistical analysis of mineral recovery

The experimental results (Table 2) revealed slight differences in chloride, sulfate, magnesium, and calcium recovery percentages throughout each variable combination. According to the data, the anions recovery varied from 3.4–14.78% and 4.21–14.91% for Cl^- and

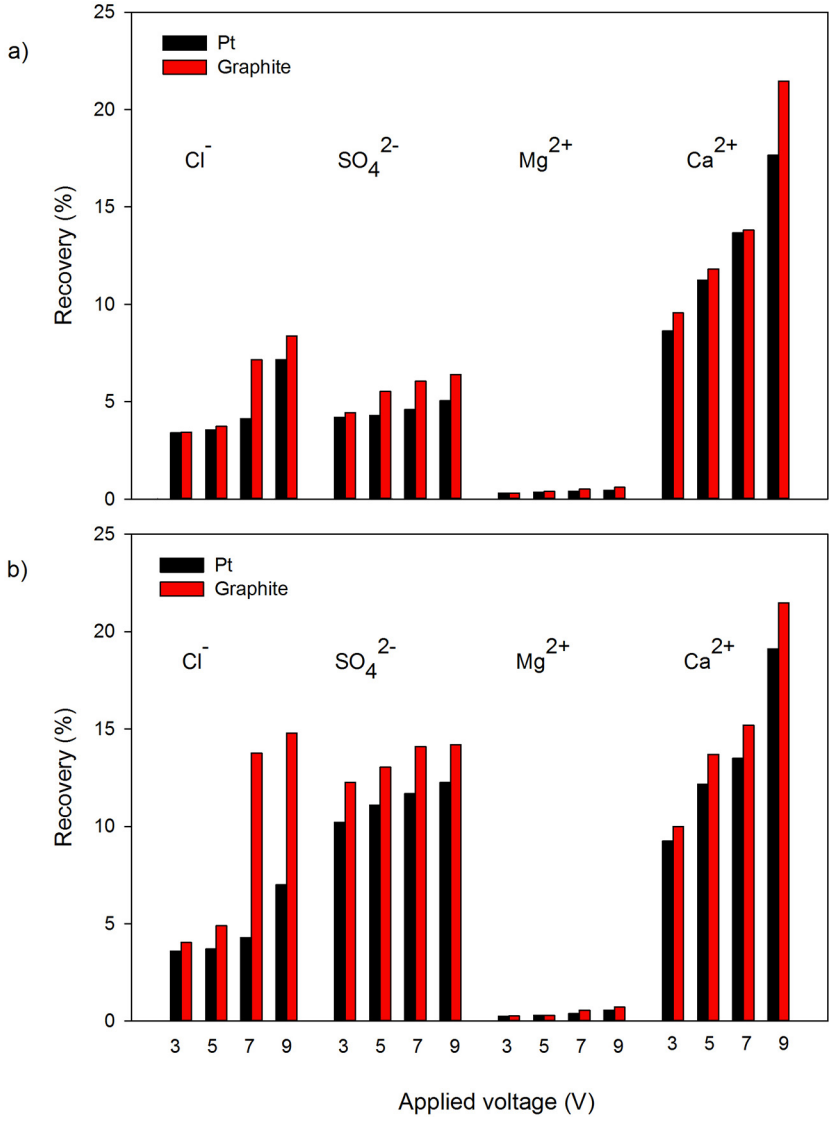

Figure 2. Electrodialytic recovery of mineral ions using Pt and graphite electrodes at a) 3-cell compartments; b) 5-cell compartments

SO_4^{2-}, respectively. Meanwhile, the cations recovery ranged from 0.25–0.72% for Mg^{2+} and 8.63–21.48% for Ca^{2+}. The highest percentage recoveries of Cl^- (14.78%), SO_4^{2-} (14.19%), Mg^{2+} (0.72%), and Ca^{2+} (21.48%) were achieved at a 5-cell reactor using a graphite electrode and 9 V of voltage. While the minimum percentages of recovery were mainly obtained at a 3-cell reactor using a Pt electrode and 3 V of voltage.

A D-optimal design was then used to determine the independent factor's effects and interactions. The obtained results were then evaluated using the sequential model sum of squares test and model summary statistics. By focusing on the maximum adjusted R^2 (adj. R^2) and predicted R^2 (pred. R^2), it was found that each response may fit a different model (Table 3). As observed, the quartic model of all responses was found to be aliased; thereby, it cannot accurately fit the design. For this reason, this study uses the suggested models (i.e., linear, linear, 2FI, and cubic) to describe the effects of cell number, applied voltage, and electrode type on the simultaneous removal of Cl^-, SO_4^{2-}, Mg^{2+}, and Ca^{2+}. The coded mathematical equations of those polynomial models can be expressed using the following equations:

- Linear

$$Y_1 = f(x) = \beta_0 + \sum_{i=1}^{k} \beta_i X_i + \varepsilon \tag{2}$$

- 2FI

$$Y_1 = f(x) = \beta_0 + \sum_{i=1}^{k} \beta_i X_i + \sum_{i=1}^{k} \sum_{j=i+1}^{k} \beta_{ij} X_i X_j + \varepsilon \tag{3}$$

- Cubic

$$Y_1 = f(x) = \beta_0 + \sum_{i=1}^{k} \beta_i X_i + \sum_{i=1}^{k} \sum_{j=i+1}^{k} \beta_{ij} X_i X_j + \sum_{i=1}^{k} \beta_{ii} X_i^2 + \sum_{i=1}^{k} \sum_{j=i+1}^{k} \beta_{iij} X_i^2 X_j + \sum_{i=1}^{k} \sum_{j=i+1}^{k} \beta_{ijj} X_i X_j^2 + \sum_{i=1}^{k} \sum_{j=i+1}^{k} \sum_{k=j+1}^{k} \beta_{ijk} X_i X_j X_k + \sum_{i=1}^{k} \beta_{iii} X_i^3 + \varepsilon \tag{4}$$

Table 2. Design of experiments

Runs	Independent variables			Experimental responses			
	x_1: Applied voltage (V)	x_2: Cell number	x_3: Electrode type	y_1: Cl^- (%)	y_2: SO_4^{2-} (%)	y_3: Mg^{2+} (%)	y_4: Ca^{2+} (%)
1	9	5	Pt	6.99	12.25	0.56	19.11
2	5	3	graphite	3.40	5.53	0.40	11.82
3	3	5	Pt	3.60	10.21	0.25	9.24
4	9	5	graphite	14.78	14.19	0.72	21.48
5	7	3	graphite	7.16	6.05	0.52	13.81
6	5	3	Pt	3.56	4.30	0.36	11.24
7	7	5	Pt	4.29	11.69	0.39	13.50
8	9	5	graphite	14.00	14.00	0.70	21.00
9	3	5	graphite	4.03	12.25	0.26	10.00
10	7	5	graphite	13.76	14.10	0.56	15.19
11	3	5	graphite	4.00	12.00	0.26	9.50
12	9	3	graphite	8.38	6.40	0.61	21.45
13	3	3	Pt	3.40	4.21	0.31	8.63
14	5	5	graphite	4.90	13.03	0.29	13.70
15	9	5	Pt	8.22	10.73	0.50	18.11
16	5	5	Pt	4.90	13.03	0.29	13.70
17	9	3	Pt	5.92	5.05	0.45	17.65
18	7	3	Pt	4.14	4.60	0.41	13.68
19	3	3	graphite	3.44	4.44	0.32	9.56
20	3	5	Pt	5.10	11.25	0.30	9.00

Table 3. Fit summary of responses

Responses	Suggested			Aliased		
	Model	Adj. R^2	Pred. R^2	Model	Adj. R^2	Pred. R^2
Cl^-	Linear	0.7738	0.7149	Quartic	0.8787	0.3973
SO_4^{2-}	Linear	0.9757	0.9686	Quartic	0.9770	0.4374
Mg^{2+}	2FI	0.9261	0.9035	Quartic	0.9627	0.2052
Ca^{2+}	Cubic	0.9801	0.9085	Quartic	0.9848	0.2767

where: Y is the predicted response;
k is the number of design factors;
β_0 is the constant coefficient;
β_i is the linear term;
β_{ij}, β_{iij}, β_{ijj}, β_{ijk} are the coefficient interaction, β_{ii}, β_{iii} are the quadratic and cubic terms, respectively;
X_i and X_j are an independent factor;
X_i^2 and X_i^3 are the quadratic and cubic terms of the factors;
ε is the error term.

Subsequently, regression analysis and ANOVA were performed according to the suggested models. The Cl^-, SO_4^{2-}, Mg^{2+}, and Ca^{2+} model terms were all highly significant (confirmed by a p-value of < 0.0001 and F-value of 22.67, 254.98, 40.68, and 86.07, respectively). In contrast, the lack of fit of the developed models was not significant, showed by the p-value of 0.3140 (Cl^-), 0.4933 (SO_4^{2-}), 0.2032 (Mg^{2+}), and 0.1591 (Ca^{2+}). This non-significant lack of fit is crucial for the model to smoothly fit. Furthermore, the coefficient of determination (R^2) assesses the proportion of variation explained by the model relative to the mean of the response (Anderson and Whitcomb, 2017). A value of R^2 over 0.9 is said to be highly correlated. However, this value may exhibit a statistical bias, particularly when the model is built based on a relatively small sample size (Anderson and Whitcomb, 2017). As an alternative, the adj. R^2 could provide a more accurate fit measure than R^2 since it reflects the number of factors involved in the model. Based on the statistical fitting (Table 4), the adjusted R^2 of all responses was between 77–98%, indicating a strong significance of the model to fit the experimental data and predict the response value. The predicted R^2 values of all models agreed with adj R^2 (indicated by the difference value < 0.2). Adequate precision is measured by dividing the maximum and the minimum predicted response by the mean standard deviation of predicted responses (Montgomery, 2013). In our study, the adequate precision of all models exceeded 4, which is desirable and indicates an adequate signal-to-noise ratio.

The effects of the independent factors on the responses are described in Table 5. The significant value of the coefficient indicates a substantial contribution to the recovery of targeted minerals. As observed, the p-value of linear coefficients (applied voltage, cell number, and electrode type) was significant to the recovery of all targeted mineral ions. The linear coefficient of cell number and electrode type was found insignificant except for magnesium and calcium recovery.

Meanwhile, the coefficient of interaction between x_1x_2 (applied voltage and cell number) and x_1x_3 (applied voltage and electrode

Table 4. Fit statistic of the developed model

Statistical parameter	Responses			
	Cl^-	SO_4^{2-}	Mg^{2+}	Ca^{2+}
St. Dev	0.0373	0.1035	0.0402	0.6170
Mean	0.1960	3.01	0.4230	14.07
C.V (%)	19.02	3.44	9.51	4.39
R^2	0.8095	0.9795	0.9728	0.9916
Adj R^2	0.7738	0.9757	0.9261	0.9801
Pred R^2	0.7149	0.9686	0.9035	0.9085
Adeq. Prec	14.6633	37.4610	19.2969	26.6339

Note: St. Dev – standard deviation; Adj R^2 – adjusted R^2; Pred R^2 – predicted R^2; Adeq. Prec – adequate precision.

type) indicated a highly significant effect on magnesium recovery. Likewise, the interaction coefficient between x_1x_3 (applied voltage and electrode type), the quadratic coefficient of applied voltage, the interaction between $x_1^2 x_3$ (the quadratic coefficient of applied current and the linear coefficient of electrode type), and the cubic coefficient of applied voltage showed significant model terms to the calcium recovery. The polynomial regression equation for mineral ions recovery in terms of actual factors can be written in Table 6.

Table 5. The effect of individual factor and their interaction with the responses

Source	Prob. F (*p*-value) < 0.05							
	Cl^- (%)		SO_4^{2-} (%)		Mg^{2+} (%)		Ca^{2+} (%)	
Model	Linear		Linear		2FI		Cubic	
x_1: Voltage	< 0.0001	*	0.0014	*	< 0.0001	*	0.0444	*
x_2: Cell number	0.0055	*	< 0.0001	*	0.9645	**	0.0154	*
x_3: Electrode type	0.0277	*	< 0.0001	*	0.0007	*	0.4020	**
$x_1 x_2$					0.0092	*	0.6615	**
$x_1 x_3$					0.0009	*	0.0129	*
$x_2 x_3$					0.9291	**	0.7227	**
x_1^2							0.0036	*
$x_1 x_2 x_3$							0.8480	**
$x_1^2 x_2$							0.1129	**
$x_1^2 x_3$							0.0510	**
x_1^3							0.0018	*

Note: * – significant; ** – not significant.

Table 6. The regression equation for mineral ions recovery

Responses	x_2	x_3	Actual equations
Cl^-	3-cells	Pt	$\frac{1}{0.398340 - 0.024918 \cdot x_1}$
		graphite	$\frac{1}{0.398340 - 0.024918 \cdot x_1}$
	5-cells	Pt	$\frac{1}{0.343823 - 0.024918 \cdot x_1}$
		graphite	$\frac{1}{0.303479 - 0.024918 \cdot x_1}$
SO_4^{2-}	3-cells	Pt	$\sqrt{1.90256 + 0.037073 \cdot x_1}$
		graphite	$\sqrt{2.14399 + 0.037073 \cdot x_1}$
	5-cells	Pt	$\sqrt{3.17279 + 0.037073 \cdot x_1}$
		graphite	$\sqrt{3.41422 + 0.037073 \cdot x_1}$
Mg^{2+}	3-cells	Pt	$0.259707 + 0.020466 \cdot x_1$
		graphite	$0.147293 + 0.052534 \cdot x_1$
	5-cells	Pt	$0.114716 + 0.044492 \cdot x_1$
		graphite	$0.005635 + 0.076561 \cdot x_1$
Ca^{2+}	3-cells	Pt	$-13.75433 + 12.91093 \cdot x_1 - 2.21250 \cdot x_1^2 + 0.130069 \cdot x_1^3$
		graphite	$-9.76608 + 11.35393 \cdot x_1 - 2.04875 \cdot x_1^2 + 0.130069 \cdot x_1^3$
	5-cells	Pt	$-16.57286 + 14.42105 \cdot x_1 - 2.34094 \cdot x_1^2 + 0.130069 \cdot x_1^3$
		graphite	$-12.50819 + 12.81631 \cdot x_1 - 2.17719 \cdot x_1^2 + 0.130069 \cdot x_1^3$

Note: x_1 – applied voltage; x_2 – cell number; x_3 – electrode type.

Model adequacy

In addition, an adequacy check was performed to validate the developed model. Model validation is required to prevent poor or misleading results from the analysis (Box et al., 1978). Figure 3 illustrates the plot of residuals versus the predicted responses, the graph of predicted

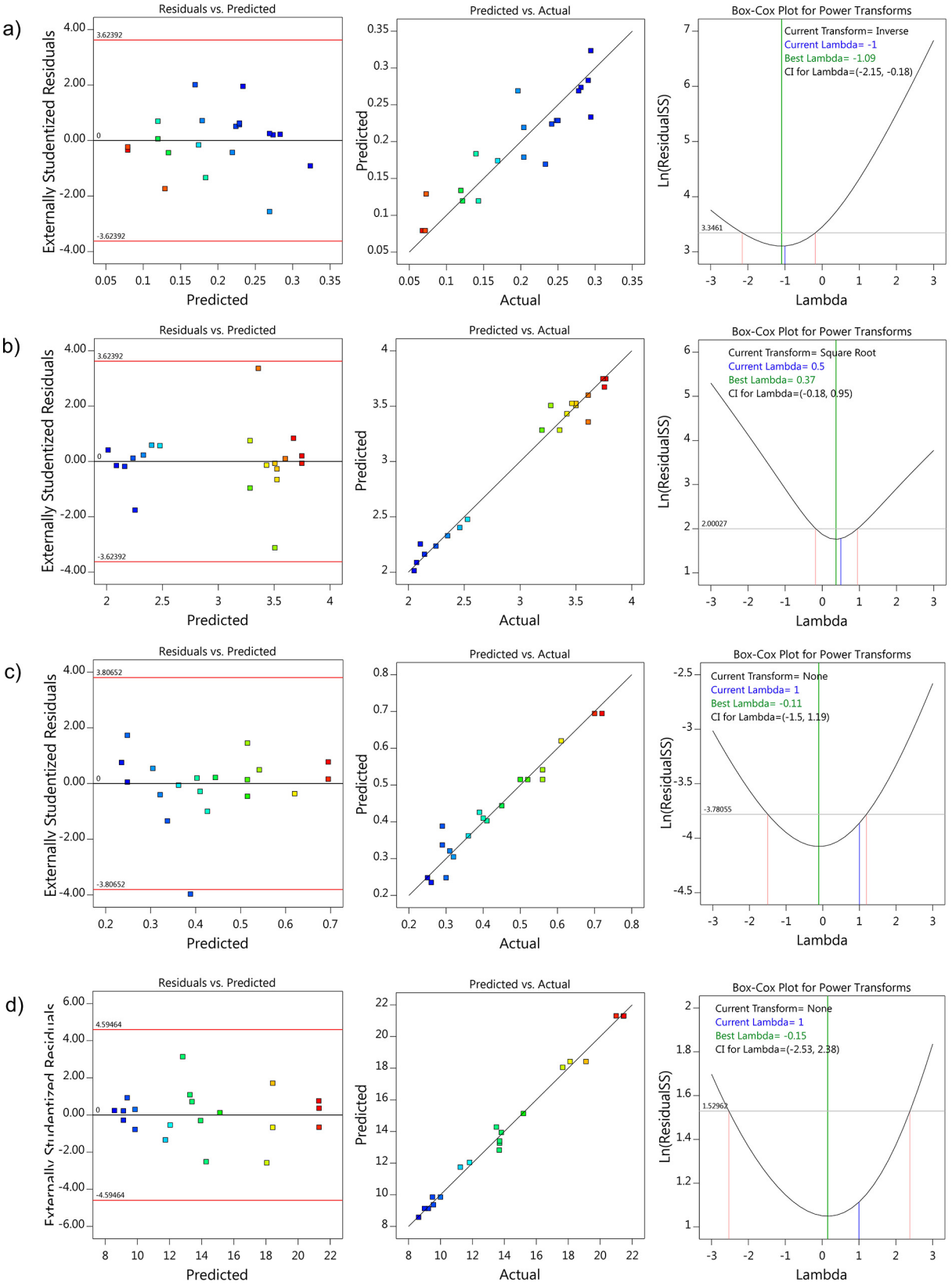

Figure 3. Model adequacy plots of a) Cl^-, b) SO_4^{2-}, c) Mg^{2+}, and d) Ca^{2+} recovery

responses versus the actual responses, and the box-cox plot for power transform. It can be seen that a random scatter was found in all the plots of residuals versus the predicted responses. A constant range of residuals was distributed across the graph and around the zero line up to a value of 3.62–4.59, suggesting a good linear relationship between residual and predicted response. An outlier was found in the residual plot of magnesium recovery. However, it does not deviate significantly from the normal pattern of the entire data set.

The graph of predicted responses versus the actual responses aims to identify a group of responses that are not easily predicted by the model. It can be seen that all points are close to the fitted line and have a narrow confidence band, which is considered a good fit for the model. Meanwhile, it can also be observed that some models (i.e., chloride and sulfate recovery) went through a box-cox plot transformation to improve their statistical analysis and diagnostic plots. As illustrated, chloride and sulfate recovery models (Fig. 3 a–b) were transformed into inverse and square root transformations, respectively, which are the closest to the best lambda (λ) value and within the confidence interval (CI). In contrast, the magnesium and calcium recovery model (Fig. 3 c–d) did not require any transformation since the lambda (λ) optimal values already lie between two pink limit lines, i.e., 3.806 to –3.806 for Mg^{2+} recovery, and 4.594 to –4.594 for Ca^{2+} recovery.

Optimization of responses

The optimization process searches for a combination of factors that can meet each factor's desired criteria and responses. Numerical optimization was applied to search the factor space for the best trade-offs to achieve multiple goals. All individual factors were set "as in range" with the same weight and importance level. Meanwhile, the responses were set as "maximize" to optimize the mineral ion recovery. The ideal desirability function is 1 (Montgomery 2013). According to the result, optimal recovery can be achieved using 5-cell compartments and 9 V voltage with a graphite electrode. As seen in Figure 4, the highest desirability value of Cl^-, SO_4^{2-}, Mg^{2+}, and Ca^{2+} recovery was 0.967. An additional experiment was performed based on the optimal scenario to verify the predicted result (Table 7).

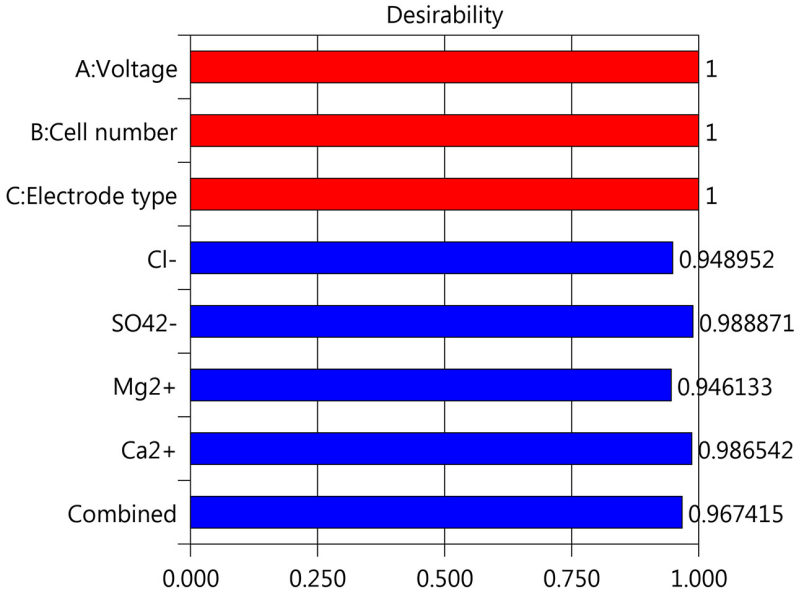

Figure 4. Desirability graph

Table 7. The validation test result of the optimum condition

Independent factors			Predicted responses				Actual responses			
Applied Voltage (V)	Cells number	Electrode type	Cl^- (%)	SO_4^{2-} (%)	Mg^{2+} (%)	Ca^{2+} (%)	Cl^- (%)	SO_4^{2-} (%)	Mg^{2+} (%)	Ca^{2+} (%)
9	5	Gr	14.62	14.05	0.69	21.30	14.39	14.10	0.70	21.24

CONCLUSION

This study evaluated the simultaneous recovery of mineral ions from bittern wastewater with the electrodialysis process. These results showed that the percentage of recovered minerals was quite small due to unaccounted precipitates that may be deposited in the electrodes or ion exchange membranes. The statistical analyses of mineral recovery were determined using the D-optimality design approach. The minerals recovery was correspondingly fit into linear (for Cl^-), linear (for SO_4^{2-}), 2FI (for Mg^{2+}), and cubic polynomial models (for Ca^{2+}) with adjusted R^2 between 77–98% and p-value < 0.001. The results illustrated that the linear coefficient of the applied voltage was highly significant to the responses. The linear coefficient of cell number and electrode type was also significant to the responses, except for magnesium and calcium.

Acknowledgments

The authors gratefully acknowledge financial support from the Institut Teknologi Sepuluh Nopember for the project scheme of the Publication Writing and IPR Incentive Program (PPHKI) 2023. The authors also acknowledge PT. Susanti Megah for the research collaboration.

Funding

The authors gratefully acknowledge financial support from the Institut Teknologi Sepuluh Nopember for this work under the project scheme of the Publication Writing and IPR Incentive Program (PPHKI) 2023.

REFERENCES

1. Agresti A. 2002. Categorical Data Analysis, 2nd edn. John Wiley & Sons, Inc., New Jersey
2. American Public Health Association. 2005. Standard Methods for The Examination of Water and Wastewater, 21st edn. American Public Health Association, American Water Works Associations, Water Environment Federation, Washington D.C., USA
3. Anderson M.J., Whitcomb P.J. 2017. RSM Simplified: Optimizing Processes Using Response Surface Methods for Design of Experiments, 2nd edn. CRC Press, Taylor & Francis Group, Florida
4. Ariono D., Purwasasmita M., Wenten I.G. 2016. Brine effluents: Characteristics, environmental impacts, and their handling. Journal of Engineering and Technological Science, 48, 367–387. https://doi.org/10.5614/j.eng.technol.sci.2016.48.4.1
5. Bagastyo A.Y., Anggrainy A.D., Gatneh S., et al. 2022. Study on optimization of coagulation-flocculation of fish market wastewater using bittern coagulant - response surface methodological approach. Water Science and Technology, 85, 3072–3087. https://doi.org/10.2166/wst.2022.136
6. Bagastyo A.Y., Sari P.P.I., Direstiyani L.C. 2021a. Effect of chloride ions on the simultaneous electrodialysis and electrochemical oxidation of mature landfill leachate. Environmental Science and Pollution Research, 28, 63646–63660. https://doi.org/10.1007/s11356-020-11519-z
7. Bagastyo A.Y., Sinatria A.Z., Anggrainy A.D., et al. 2021b. Resource recovery and utilization of bittern wastewater from salt production: A review of recovery technologies and their potential applications. Environmental Technology Reviews, 10, 294–321. https://doi.org/10.1080/21622515.2021.1995786
8. Barakwan R.A., Hardina T.T., Trihadiningrum Y., Bagastyo A.Y. 2019. Recovery of alum from Surabaya water treatment sludge using electrolysis with carbon-silver electrodes. Journal of Ecological Engineering, 20, 126–133. https://doi.org/10.12911/22998993/109861
9. Box G.E.P, Hunter W.G., Hunter J.S. 1978. Statistics For Experimenter: An Introduction to Design, Data Analysis and Model Building. John Wiley & Sons, Inc., USA
10. Dave R.H., Ghosh P.K. 2005. Enrichment of bromine in sea-bittern with recovery of other marine chemicals. Industrial and Engineering Chemistry Research, 44, 2903–2907. https://doi.org/10.1021/ie049130x
11. Einav R., Harussi K., Perry D. 2002. The footprint of the desalination processes on the environment. Desalination, 152, 141–154. https://doi.org/10.1016/S0011-9164(02)01057-3
12. Gacia E., Invers O., Manzanera M., et al. 2007. Impact of the brine from a desalination plant on a shallow seagrass (Posidonia oceanica) meadow. Estuarine Coastal and Shelf Science, 72, 579–590. https://doi.org/10.1016/j.ecss.2006.11.021
13. Hikmawati D.N., Bagastyo A.Y., Warmadewanthi I. 2019. Electrodialytic recovery of ammonium and phosphate ions in fertilizer industry wastewater by using a continuous-flow reactor. Journal of Ecological Engineering, 20, 255–263. https://doi.org/10.12911/22998993/109461
14. Honarparvar S., Reible D. 2020. Modeling multicomponent ion transport to investigate selective ion removal in electrodialysis. Environmental Science and Ecotechnology, 1, 100007. https://doi.org/10.1016/j.ese.2019.100007

15. Kartika S.W.T., Bagastyo A.Y. 2022. Recovery of Ca^{2+} and SO_4^{2-} from bittern wastewater using electrodialysis method. IOP Conference Series: Earth and Environmental Science, 1095, 012029. https://doi.org/10.1088/1755-1315/1095/1/012029
16. Mohammadi R., Tang W., Sillanpää M. 2021. A systematic review and statistical analysis of nutrient recovery from municipal wastewater by electrodialysis. Desalination, 498, 114626. https://doi.org/10.1016/j.desal.2020.114626
17. Montgomery D.C. 2013. Montgomery Design and Analysis of Experiments Eighth Edition. Arizona State University, 8th edn. John Wiley & Sons, Inc., USA
18. Nie X.Y., Sun S.Y., Sun Z., et al. 2017. Ion-fractionation of lithium ions from magnesium ions by electrodialysis using monovalent selective ion-exchange membranes. Desalination, 403, 128–135. https://doi.org/10.1016/j.desal.2016.05.010
19. Panagopoulos A., Haralambous K.J. 2020. Environmental impacts of desalination and brine treatment - Challenges and mitigation measures. Marine Pollution Bulletin, 161, 111773. https://doi.org/10.1016/j.marpolbul.2020.111773
20. Roberts D.A., Johnston E.L., Knott N.A. 2010. Impacts of desalination plant discharges on the marine environment: A critical review of published studies. Water Research, 44, 5117–5128. https://doi.org/10.1016/j.watres.2010.04.036
21. Strathmann H. 1986. Electrodialysis. In: Bungay PM, Lonsdale HK, DePinho MN (eds) Synthetic Membranes: Science, Engineering and Applications. Springer, Dordrecht
22. Tovar L.R., Gutierrez M.E., Cruz G. 2002. Fluoride content by ion chromatography using a suppressed conductivity detector and osmolality of bitterns discharged into the pacific ocean from a saltworks: feasible causal agents in the mortality of green turtles (Chelonia mydas) in the Ojo de Liebre lagoon, Baja California Sur, Mexico. Analytical Science, 18, 1003–1007. https://doi.org/10.2116/analsci.18.1003
23. Wang Y., Huang C., Xu T. 2010. Optimization of electrodialysis with bipolar membranes by using response surface methodology. Journal of Membrane Science, 362, 249–254. https://doi.org/10.1016/j.memsci.2010.06.049
24. Ye Z.L., Ghyselbrecht K., Monballiu A., et al. 2018. Fractionating magnesium ion from seawater for struvite recovery using electrodialysis with monovalent selective membranes. Chemosphere, 210, 867–876. https://doi.org/10.1016/j.chemosphere.2018.07.078
25. Zhang Y., Wang L., Sun W., et al. 2020. Membrane technologies for Li^+/Mg^{2+} separation from salt-lake brines and seawater: A comprehensive review. Journal of Industrial and Engineering Chemistry, 81, 7–23. https://doi.org/10.1016/j.jiec.2019.09.002